



Published in final edited form as:

Neurogastroenterol Motil. 2021 September ; 33(9): e14149. doi:10.1111/nmo.14149.

Bicarbonate Ion Transport by the Electrogenic $\text{Na}^+/\text{HCO}_3^-$ Cotransporter, NBCe1, is Required for Normal Electrical Slow Wave Activity in Mouse Small Intestine

Wenchang Zhao^{1,2,4,#}, Liwen Zhang^{1,2,4,#}, Leonid G. Ermilov^{1,2}, Maria Gabriela Colmenares Aguilar^{1,2}, David R. Linden^{1,2}, Seth T. Eisenman^{1,2}, Michael F. Romero^{2,3}, Gianrico Farrugia^{1,2}, Lei Sha^{4,†}, Simon J. Gibbons^{1,2,†}

¹Enteric Neuroscience Program, Division of Gastroenterology and Hepatology, Rochester, Minnesota, USA.

²Physiology and Biomedical Engineering, Rochester, Minnesota, USA.

³Division of Nephrology and Hypertension, Mayo Clinic, Rochester, Minnesota, USA.

⁴Neuroendocrine Pharmacology, China Medical University, Shenyang, Liaoning Province, P. R. China.

Abstract

Background: Normal gastrointestinal motility depends on electrical slow wave activity generated by interstitial cells of Cajal (ICC) in the tunica muscularis of the gastrointestinal tract. A requirement for HCO_3^- in extracellular solutions used to record slow waves indicates a role for HCO_3^- transport in ICC pacemaking. The *Slc4a4* gene transcript encoding the electrogenic $\text{Na}^+/\text{HCO}_3^-$ co-transporter, NBCe1, is enriched in mouse small intestinal myenteric region ICC (ICC-MY) that generate slow waves. This study aimed to determine how extracellular HCO_3^- concentrations affect electrical activity in mouse small intestine and to determine the contribution of NBCe1 activity to these effects.

Key Results: NBCe1 immunoreactivity was localized to ICC-MY of the tunica muscularis. In sharp electrode electrical recordings, removal of HCO_3^- from extracellular solutions caused significant, reversible, depolarization of the smooth muscle and a reduction in slow wave amplitude and frequency. In 100mM HCO_3^- , the muscle hyperpolarized and slow wave amplitude and frequency increased. The effects of replacing extracellular Na^+ with Li^+ , an ion that does not support NBCe1 activity, were similar to, but larger than, the effects of removing HCO_3^- . There were no additional changes to electrical activity when HCO_3^- was removed from Li^+ containing solutions. The $\text{Na}^+/\text{HCO}_3^-$ co-transport inhibitor, S-0859 (30 μM) significantly reduced the effect of removing HCO_3^- on electrical activity.

[†] Corresponding Authors: Simon J Gibbons, Ph.D., Enteric Neuroscience Program, Division of Gastroenterology and Hepatology, Mayo Clinic, Rochester, MN, 55905, USA. gibbons.simon@mayo.edu. Telephone: +1 507 284 9652, Lei Sha, M.D., China Medical University, 77 Pu He Road, Shenbei New District, Shenyang, Liaoning Province, P. R. China, 110122, lsha@cmu.edu.cn, lei.sha@foxmail.com. Telephone: +86 18900911003.

[#] These authors contributed equally to this work.

Conclusions: These studies demonstrate a major role for $\text{Na}^+/\text{HCO}_3^-$ cotransport by NBCe1 in electrical activity of mouse small intestine and indicated that regulation of intracellular acid:base homeostasis contributes to generation of normal pacemaker activity in the gastrointestinal tract.

Keywords

Interstitial Cells of Cajal; Gastrointestinal Motility; Slc4a4 protein; mouse; Muscle; Smooth; Intestine; Small; Pacemakers; Biological

INTRODUCTION

Gastrointestinal motility depends on patterns of smooth muscle contractions driven by rhythmic electrical activity known as electrical slow waves. These slow waves are generated by interstitial cells of Cajal (ICC)¹⁻³, which are mesoderm-derived mesenchymal cells distributed throughout the tunica muscularis of the vertebrate gastrointestinal tract⁴⁵. ICC have other functions in addition to electrical pacemaking including setting the membrane potential gradients across the smooth muscle layers⁶, mediating neuromuscular signaling⁷⁻⁹ and acting as mechanosensors^{10, 11}. The central role of ICC in gastrointestinal function is indicated by the effect of depleted ICC networks on gastrointestinal motility in animal models^{2, 3, 12-14} and the demonstration that tissues from patients with motility disorders including diabetic gastroparesis and slow transit constipation are depleted of ICC¹⁵⁻¹⁸. In patients with diabetic gastroparesis and diabetic mice with delayed gastric emptying, irregular patterns of slow wave propagation are linked to depletion of ICC¹⁹.

The molecular determinants for the diversity of ICC functions, and variations in the shape and frequency of slow wave activity throughout the gastrointestinal tract have not been fully elucidated. The basic model is that generation of electrical slow wave activity by ICC depends upon multiple factors that couple large, regular transient rises in cytosolic Ca^{2+} concentrations to oscillations in membrane potential. The process is dependent on release of Ca^{2+} into the cytosol from inositol 1,4,5-trisphosphate (IP3)-sensitive intracellular stores²⁰, which is coupled to influx of Ca^{2+} through voltage gated Ca^{2+} channels^{21,22} and non-selective cation channels including Ca^{2+} release activated channels such as *orai*²³, followed by activation of Anoctamin-1 (Ano1, TMEM16A) Ca^{2+} -sensitive Cl^- channels²⁴⁻²⁶. Mitochondrial buffering of cytosolic Ca^{2+} ²⁷, the activity of $\text{Na}^+/\text{Ca}^{2+}$ exchangers (NCX)²⁸ and reuptake of Ca^{2+} into the endoplasmic reticulum²⁷ alter the shape and duration of the Ca^{2+} transients and the associated electrical slow wave. Plasma membrane transporters of Cl^- ions including NKCC1 (Slc12a2) set the Cl^- reversal potential (E_{Cl}), and E_{Cl} determines the voltage to which the ICC membrane potential depolarizes during the plateau phase of the electrical slow wave²⁹. Studies on the size and coordination of slow waves in an electrically coupled network are necessary because these factors likely determine the efficiency with which organized smooth muscle contractility is engaged and maintained to ensure normal motility.

Many of the processes listed above are sensitive to regulation by pH^{30,31,32,33} but although the contractility patterns and electrical activities of the vertebrate gastrointestinal tract are modified by changing extracellular pH and HCO_3^- ^{34, 35}, the mechanisms for pH

regulation in ICC have not been specifically investigated. Interestingly, transcriptomic profiling of mouse intestinal ICC identified enrichment of *Slc4a4* transcripts in myenteric ICC (ICC-MY), which generate pacemaker activity, but ICC from the deep muscular plexus (ICC-DMP), which are not pacemaker cells³⁶, express lower levels of *Slc4a4* mRNA. *Slc4a4* encodes the electrogenic Na⁺/HCO₃⁻ co-transporter, NBCe1, a protein that regulates absorption and secretion of bicarbonate and carbonate, and contributes to intracellular pH homeostasis³⁷. Variants of NBCe1³⁷ are widely expressed in tissues that transport bulk quantities of HCO₃⁻ including renal proximal tubules³⁷ but also excitable cells in the central nervous system and heart³⁸⁻⁴⁰. As an electrogenic transporter with a predicted inward stoichiometry of two negative charges for each positive Na⁺ ion carried in physiological solutions⁴¹, NBCe1 activity can contribute to the membrane potential of excitable cells and as a carrier of HCO₃⁻/CO₃²⁻ ions, it can modify various signaling pathways through alteration of intracellular pH. Gene targeted *Slc4a4* knockout mice die young due to metabolic acidosis⁴² but small molecule inhibitors of NBCe1 are available, including S-0859, which selectively inhibits NBCe1 at concentrations that do not significantly affect other related plasma membrane transport proteins including NKCC1 and NCX proteins^{43,44,45}.

The aim of this study was to test the hypothesis that altered extracellular HCO₃⁻ levels modify mouse small intestinal electrical activity and that NBCe1 activity contributes to the effects of changes in HCO₃⁻. We found that NBCe1 protein is enriched in pacemaker ICC-MY and that changes in electrical activity in response to altering extracellular HCO₃⁻ levels were consistent with direct effects on ICC excitability due to NBCe1 activity.

MATERIALS AND METHODS

Animals:

Adult (six weeks or older) C57Bl/6J mice of either sex (Jackson, Bar Harbor, ME, USA) used in this study were maintained and experiments done with the approval of the Institutional Animal Care and Use Committee of the Mayo Clinic (Rochester MN USA) under protocol number A00002343-16. Mice had free access to food and water and were checked daily. Mice were killed by CO₂ inhalation followed by cervical dislocation.

Tissue preparation:

Tissues were prepared and recordings made using a previously reported method⁴⁶. Briefly, segments of jejunum were removed into Krebs solution (KRB – solution ① in Table 1) and muscle strips were prepared. After pinning out onto recording chambers, tissues were placed in the setup and superfused with KRB solution ① at 37°C gassed with 97% O₂: 3% CO₂, then allowed to equilibrate prior to starting an experiment. Recordings were made using microelectrodes filled with 3M KCl with 70–90MΩ tip resistances and collected at a sampling rate of 5kHz. Bath electrodes were grounded through an agarose salt bridge made with 3M KCl to avoid junction potentials.

Solutions and chemicals:

Table 1 lists the recording solutions, which were warmed to $37\pm 1^\circ\text{C}$ and aerated to achieve a stable pH of 7.35–7.45 using gasses containing CO_2 levels chosen to equilibrate HCO_3^- levels at the desired levels at this temperature and pH. To buffer HCO_3^- -free solutions, we added 15mM HEPES and adjusted the pH to 7.4 using NaOH. To exclude the influence of HEPES on electrical activity, 15mM HEPES was included in all other solutions. pH was adjusted after equilibration by gassing at 37°C and osmolarity of the solutions was confirmed to be $310\pm 5\text{mOsm L}^{-1}$ at equilibrium using a freezing point osmometer. The L-type Ca^{2+} channel inhibitor nifedipine ($2\mu\text{M}$, Sigma-Aldrich, St Louis, MO, USA) and the myosin light chain kinase inhibitor ML-7 ($5\mu\text{M}$, Cayman Chemicals, Ann Arbor, MI, USA) were used to minimize smooth muscle contractility and maintain stable impalements. Electrical activity recorded in the presence of ML-7 was not different from that previously recorded in nifedipine alone⁴⁶ and removing HCO_3^- in the absence of ML-7 produced similar effects to that reported in this manuscript in $n = 4$ cells from $N = 3$ mice. S-0859 was obtained from Cayman, unless otherwise indicated reagents were from Sigma-Aldrich.

Data analysis

Data were analyzed offline using Clampfit 10.7 (Molecular Devices). Spontaneous electrical activity was accepted for analysis as a slow wave if the peak amplitude was $>3\text{mV}$. Slow wave properties were determined by analyzing 30 seconds of data when the activity was at steady state or immediately prior to solution change and averaging the electrical properties for all of the events occurring in that time. The following properties were determined: (i) resting membrane voltage at the most hyperpolarized point of the slow wave, (ii) slow wave amplitude from the resting membrane potential to the peak of the next action potential, (iii) slow wave duration (or width) at 50% of peak amplitude, (iv) rise time was the time between 10% and 90% of peak amplitude, and (v) slow wave frequency was the reciprocal of the inter-event interval (peak to peak).

Immunolabeling for NBCe1

Whole thickness preparations of tunica muscularis from the proximal small intestine with intact myenteric ICC (ICC-MY), and deep muscular plexus ICC (ICC-DMP) were prepared after excision from the animal, pinning onto Petri dishes lined with Sylgard (Dow Corning, Midland, MI, USA), and separation of the muscle from the mucosa by peeling. After overnight fixation in cold, 4% paraformaldehyde in 0.1M phosphate buffer (pH 7.2), and washing in 0.1M phosphate buffered saline (PBS, 8×15 min), tissues were permeabilized and blocked in 1% bovine serum albumin (BSA) in PBS plus 0.3% Triton-X-100 in PBS (4 h at room temperature). Primary antibodies were added in 1% BSA, PBS plus 0.3% Triton-X-100 and incubated for 48h at 4°C . To detect NBCe1, we used a rabbit anti-Slc4a4 antibody (Catalog # 11885-1-AP, RRID AB_2191458) from Proteintech (Rosemont IL, USA) diluted to 0.3mg ml^{-1} . ICC were identified by doubly labeling using a goat anti-Kit antibody (Catalog # AF 1356, RRID AB_354750) from R&D Systems (Minneapolis, MN, USA) diluted to 0.2mg ml^{-1} . The tissue was washed with PBS 8×30 minutes then incubated overnight in the dark with the following secondary antibodies; Cy3-conjugated donkey anti-rabbit ($1.88\mu\text{g ml}^{-1}$, Cat # 711-165-152, RRID AB_2307443) and Alexa Fluor®-488-

conjugated donkey anti-goat ($3.75\mu\text{g ml}^{-1}$, Cat # 711-165-152, RRID AB_2307443) from Jackson ImmunoResearch (West Grove, PA, USA). For imaging, tissues were washed, and counterstained with DAPI dilactate (Invitrogen, Carlsbad, CA) to label nuclei then mounted in Diamond SlowFade™ mounting medium (Thermo Fisher).

Image acquisition

Images were collected with an Olympus (Center Valley, PA, USA) FV1000 laser scanning confocal microscope using a 20X 0.95NA, water-immersion objective with the confocal aperture set to give the optimal resolution for the illumination settings chosen to visualize the fluorophores. XYZ stacks were collected and 2D projections were created using the Olympus Fluoview software. The following lasers and emission filters were used: multiline Ar laser at 488nm (for Alexa Fluor 488); emission filter 535 ± 15 nm; 543nm HeNe laser (for Cy3); emission filter 575–630nm; and 405nm laser diode (used for DAPI); emission filter 430–470nm. Images were prepared using Adobe Photoshop CS. No 3D reconstructions, deconvolution, surface or volume rendering, or gamma adjustments were done to create the images.

Statistics

Data are expressed as means \pm standard deviations. Statistical significance was determined by GraphPad Prism (Graphpad Software Inc., La Jolla, CA, USA) using tests chosen based on whether the data were normally distributed and/or matched, and correcting for multiple comparisons where necessary. The text and figure legends indicate the chosen test. Means calculated from multiple recordings in a tissue from a single animal were treated as a single N value for the purposes of calculating averages, standard deviations and significance. ‘n’ indicates the number of recordings in total from all tissues.

RESULTS

The $\text{Na}^+/\text{HCO}_3^-$ cotransporter NBCe1 is expressed at higher levels in ICC-MY than in ICC-DMP of mouse small intestine.

Differences in mRNA expression between purified populations of pacemaker ICC-MY and non-pacemaker ICC-DMP in mouse small intestine have been reported³⁶. Among these lists for transcripts of ion channels and transporters that might account for the pacemaker function of ICC-MY, transcripts of the *Slc4a4* gene were enriched in ICC-MY compared to ICC-DMP. To confirm our prior work (manuscript under review) that the differential expression of mRNA associated with differences in NBCe1 protein expression, we again examined the distribution of NBCe1 in the adult mouse small intestine by immunofluorescence labeling. In confirmation of our previous results⁴⁷, NBCe1-IR is observed in Kit-positive ICC-MY, whereas ICC-DMP were Kit-positive but NBCe1-negative. A few myenteric neurons were also NBCe1-positive but were Kit-negative (Fig 1).

Removal of bicarbonate alters slow wave activity and causes depolarization of intestinal smooth muscle.

Although it is widely accepted that extracellular HCO_3^- is required to record normal electrical slow wave activity, no detailed studies have reported the role of HCO_3^- transport

in slow wave activity of the mouse small intestine. We recorded from the circular muscle layer of mouse jejunum while altering extracellular HCO_3^- levels at constant pH and temperature. We recorded typical and regular electrical slow waves in standard KRB containing 15.5mM HCO_3^- (97% O_2 , 3% CO_2). In the absence of extracellular HCO_3^- (100% O_2 , 0% CO_2 , pH buffered to 7.4 with 15mM HEPES-OH), the membrane voltage depolarized by 4.97 ± 1.96 mV in a reproducible and reversible manner, (Fig 2A, C, Supplementary Table 1, n=26 cells from N=26 mice, $P < 0.05$, repeated measures, one-way ANOVA with Tukey's post test). The decreases in slow wave amplitude (5.6 ± 2.39 mV) and frequency (0.074 ± 0.03 Hz, 4.44 ± 1.8 cpm) were also statistically significant and reversible (Fig 2B, D, E, Supplementary Table 1, n=26 cells from N=26 mice, $P < 0.05$, repeated measures, one-way ANOVA with Tukey's post test). Furthermore, slow waves were of longer duration and the rising phase of the depolarization was slower resulting in a longer time from 10%–90% of peak amplitude after removal of HCO_3^- (Fig 2B, F, G, Supplementary Table 1, n=26 cells from N=26 mice, $P < 0.05$, repeated measures, one-way ANOVA with Tukey's post test). These observations support a requirement for HCO_3^- in normal slow wave activity.

Increasing extracellular HCO_3^- to 100mM causes membrane hyperpolarization and increases slow wave amplitude.

Wienbeck reported that high CO_2 concentrations make the phase of spontaneous contractile activity longer and amplitude higher in mechanical recordings from guinea pig taenia coli³⁴. We increased extracellular HCO_3^- from 15.5mM to 100mM by substituting HCO_3^- for Cl^- to maintain the osmolarity of the solutions. These solutions were gassed with 20% CO_2 , 80% O_2 to stabilize the HCO_3^- concentrations and contained 15mM HEPES-OH with the pH adjusted to 7.4 at 37°C. In 100mM HCO_3^- , membrane potential was significantly hyperpolarized (Fig 3A, 3C) and the slow wave shape was reproducibly changed (Fig 3B). Slow waves in 100mM HCO_3^- had significantly higher amplitudes, and shorter durations based on width at half peak amplitude compared to events recorded in 15mM HCO_3^- (Fig 3A–D, F, Supplementary Table 2, n=17 cells from N=5 mice, $P < 0.05$, repeated measures, one-way ANOVA with Tukey's post-test). The frequency and the initial rise times of the events were not significantly changed on application of 100mM HCO_3^- but after switching back to a solution containing 15.5mM HCO_3^- , the slow wave frequency was significantly lower and the rise time of the events was significantly faster (Fig 3A–B, E, G, Supplementary Table 2, n=17 cells from N=5 mice, $P < 0.05$, repeated measures, one-way ANOVA with Tukey's post-test). These effects of raising extracellular HCO_3^- were the reverse of what we observed when we removed HCO_3^- from the extracellular solutions.

Replacement of extracellular Na^+ with Li^+ causes membrane potential depolarization and loss of slow wave activity.

Many Na^+ -selective ion channels and transporters are also permeable to Li^+ ions but Li^+ ions do not support electrogenic $\text{Na}^+/\text{HCO}_3^-$ co-transport⁴⁸. Therefore, we replaced 120 mM NaCl with LiCl, without changing pH, osmolarity and HCO_3^- concentration. This solution change caused rapid membrane depolarization and reduction in slow wave amplitude such that after 5 min of incubation, there was complete loss of slow wave activity in 11/19 cells (Fig 4A, N = 5 mice). Short incubations with Li^+ -containing solutions

(less than 2 min) produced fully reversible changes but after longer exposure, electrical activity remained abnormal even after prolonged washout. We quantified the effects after 80 seconds of Li^+ exposure instead of waiting for the response to reach a steady state. At 80 seconds of Li^+ exposure, membrane voltage depolarized (Fig 4A, 4C) and slow wave size, frequency and shape were significantly altered (Fig 4, Supplementary Table 3, $n=19$ cells from $N=5$ mice, repeated measures, one-way ANOVA with Tukey's post test). Slow waves in Li^+ -containing solutions had lower amplitudes, longer durations based on width at half peak amplitude, slower rise times as indicated by time from 10–90% of peak amplitude and lower frequencies. This was similar to the effect of removing HCO_3^- and was the opposite of the effect of increasing HCO_3^- in the extracellular solutions.

Removal of HCO_3^- in addition to replacement of Na^+ with Li^+ produced the same effect as replacement of Na^+ alone.

To confirm that at least part of the effect of removing Na^+ was due to prevention of $\text{Na}^+/\text{HCO}_3^-$ co-transport, we determined whether removal of HCO_3^- in a Li^+ -containing solution had any further effect on electrical activity. There was no difference in the effect of replacing Na^+ with Li^+ when HCO_3^- was also removed. Membrane potential depolarized rapidly and significantly (Fig 5A, 5C) and there was completely loss of slow waves after 5 mins of incubation. Short incubations with Li^+ -containing solutions in 0mM HCO_3^- (less than 2 min) produced fully reversible effects but after longer exposures electrical activity remained abnormal even after prolonged washout. The effects of 80 seconds of Li^+ exposure in 0mM HCO_3^- were membrane depolarization (Fig 5A, 5C) and significant changes to slow wave size and frequency (Fig 5A, 5B). Slow waves in Li^+ -containing, 0mM HCO_3^- solutions had significantly lower amplitudes and lower frequencies (Fig 5D, 5E, Supplementary Table 4, $n=14$, $N=4$, $P<0.05$, $P<0.05$, One-way ANOVA with Tukey's post-test). Slow wave durations and times to peak also decreased in a reversible manner but the overall effects were not significant when taking the averages of repeated observations from a single tissue as the N value (Fig 5F, 5G, Supplementary Table 4, $n=14$, $N=4$, $P<0.05$, $P<0.05$, One-way ANOVA with Tukey's post-test). Replacing NaCl with LiCl had the same effect in the presence or absence of HCO_3^- , as indicated by no significant differences between the magnitude of the effects on membrane voltage, peak amplitude, slow wave frequency or on slow wave rise time and slow wave duration (Supplementary Table 5).

Inhibition of NBCe1 activity with S-0859 reduces the effect of removing HCO_3^- .

NBCe1 dynamically regulates pH_i , partly due to the voltage-dependent activity of this electrogenic $\text{Na}^+/\text{HCO}_3^-$ co-transporter. We tested whether inhibition of NBCe1 activity would reduce the effects of removing extracellular HCO_3^- on electrical activity. To do this, we used a generic inhibitor of $\text{Na}^+/\text{HCO}_3^-$ co-transport, S-0859, at a concentration (30 μM) that does not block Na^+/H^+ exchange⁴³ or $\text{Na}^+/\text{Ca}^{2+}$ exchange⁴⁹. In the presence of S-0859, electrical responses to 0mM HCO_3^- solution were significantly smaller. S-0859 alone caused a small, but reproducible membrane depolarization and increase in slow wave amplitude when applied in normal Krebs Ringer solution containing 15.5mM HCO_3^- (Fig 6A, Supplementary Table 6, $n = 24$, $N = 7$, $P<0.05$, one sample Student's T test vs no effect). This suggests that NBCe1-mediated ion transport occurs under normal physiological conditions. When HCO_3^- levels were changed, membrane depolarization at 5 min in 0mM

HCO_3^- in the presence of $30\mu\text{M}$ S-0859 was significantly smaller than observed in the absence of S-0859 (Fig 6A,6C, Supplementary Table 6, $P<0.05$, t test). Furthermore, the effect on slow waves of zero HCO_3^- in S-0859-containing solutions was also reduced. The decreases in slow wave amplitudes and frequencies in response to zero HCO_3^- were reduced by an average of 51% and 69% respectively in the presence of S-0859 (Fig 6D,6E, Supplementary Table 6, $P<0.05$, t test), and the effects of removing HCO_3^- on slow wave duration and rise time were numerically smaller, but the effect did not reach significance (Supplementary Table 6). S-0859 is dissolved in DMSO, therefore we tested the effect of 0.3% DMSO on electrical activity in the mouse small intestine. We observed no significant effect of DMSO on baseline electrical activity ($n = 8$ cells from $N = 3$ mice) and a similar response to 0 HCO_3^- in the presence of DMSO ($n = 6$ cells from $N = 3$ mice) when compared to the response in the absence of DMSO.

DISCUSSION

In this study, we determined a major role for $\text{Na}^+/\text{HCO}_3^-$ cotransport by NBCe1, expressed in pacemaker ICC-MY, in normal electrical activity of mouse small intestine. We found that extracellular Li^+ , which does not support HCO_3^- transport by NBCe1 (especially rodent NBCe1), resulted in membrane potential depolarization and loss of electrical slow wave activity. We also demonstrated that S-0859, an inhibitor of NBCe1, reduced the effect of removing extracellular HCO_3^- on electrical activity.

Early studies on smooth muscle function identified effects of changing extracellular pH and/or CO_2 levels on smooth muscle tone and contractile patterns. Altering extracellular HCO_3^- and CO_2 levels modifies basal contractile tone³⁵ and rhythmic electrical activity³⁴ of gastrointestinal smooth muscle but the cellular and molecular mediators of these effects have not been identified. HCO_3^- transport also contributes to normal patterns of electrical activity in other excitable cells including central neurons and cardiac myocytes^{39,40}.

We investigated a role for NBCe1 activity in pacemaker function of ICC due to the relative enrichment of *Slc4a4* gene transcripts in ICC-MY vs ICC-DMP of mouse small intestine³⁶. Our immunolabeling results confirmed prior work that showed that the NBCe1 protein encoded by *Slc4a4* is also more highly expressed in ICC-MY than in ICC-DMP, and adjacent smooth muscle cells⁵⁰. Other Na^+ -dependent HCO_3^- transporters are not enriched in ICC-MY compared to other cells in the tunica muscularis or the ICC-DMP based on the transcriptional profiling of these cell types³⁶. Under normal physiological recording conditions in 15.5mM extracellular HCO_3^- maintained at a pH of 7.4 by gassing with 3% CO_2 and with 136.7mM extracellular Na^+ , the NBCe1 transporter will carry $\text{HCO}_3^-/\text{CO}_3^{2-}$ and Na^+ ions into the cell with a stoichiometry of 2 negative charges for each positive Na^+ ion carried⁴⁸. Thus, NBCe1 activity is electrogenic resulting in net inward transport of at least one negative charge. The smooth muscle depolarization observed when we remove HCO_3^- , and the hyperpolarization observed when we increase extracellular HCO_3^- concentrations is consistent with NBCe1 transporters driving the response to altered $\text{HCO}_3^-/\text{CO}_3^{2-}$ distribution across the plasma membrane. This change in resting membrane voltage matched the change in amplitude of the electrical slow waves resulting in smaller amplitude events in 0 HCO_3^- and larger events in 100 mM HCO_3^- . Thus, the change in

slow wave amplitude reflects an effect on the resting membrane voltage, not a change in the peak voltage of the slow wave events. ICC contribute to setting the smooth muscle membrane potential⁶ and our observations of changes in membrane potential in response to changing extracellular HCO_3^- are consistent with an effect on ICC as opposed to an effect directly on smooth muscle cells. We cannot exclude some impact on smooth muscle cells but it is clear that the smooth muscle membrane potential setpoint depends on HCO_3^- concentrations, which will be altered according to the metabolic activity of the tissue and the overall acid:base homeostasis in the organism⁵¹.

We interpret the changes to slow wave frequency and duration in response to changing HCO_3^- concentrations as direct effects on ICC. ICC-MY in the small intestine generate slow waves^{2, 3} and it is established that pharmacological and genetic approaches that also change slow wave duration and frequency, produce their effects by acting on ion channels or transporters in ICC but not in smooth muscle cells^{24, 25, 29}. Enriched expression of NBCe1 in ICC-MY indicates that altered extracellular HCO_3^- levels are coupled to changes in intracellular pH in pacemaker ICC. All cells tightly control intracellular pH in response to cytosolic acidification due to catabolism and accumulation of H^+ along its electrochemical gradient. H^+ and HCO_3^- transport finely control intracellular pH and maintain it in a range that is optimal for protein function and normal molecular interactions⁵². In addition to these homeostatic processes, dynamic changes in pH across cellular compartments also modify important cellular signaling pathways. The patterns and mechanisms for regulation of intracellular pH in ICC are not known, and there is limited information on the effects of changes in intracellular pH on ICC function. However, the underlying processes responsible for generation of pacemaker potentials depend on maintenance of the mitochondrial membrane potential (ψ_m) and functional endoplasmic reticulum Ca^{2+} storage, release and reuptake²⁷. Changes in cellular pH modify these processes, cytosolic alkalization increases Ca^{2+} release from IP₃-receptor sensitive intracellular Ca^{2+} stores^{31, 32}, enhances coupling of Ca^{2+} store activation to Orai1-mediated plasma membrane Ca^{2+} influx³³, and inhibits Ca^{2+} re-uptake into the endoplasmic reticulum by the sarco/endoplasmic reticulum Ca^{2+} -ATPase (SERCA)³³. These effects of intracellular alkalization will increase the probability and amplitude of transient Ca^{2+} release events, which in ICC means an increased frequency of the Ca^{2+} transients that underlie electrical slow waves. Mitochondrial Ca^{2+} buffering is enhanced in response to cytosolic alkalization by favoring $\text{H}^+/\text{Ca}^{2+}$ exchange across the inner mitochondrial membrane^{53, 54}. This effect will shorten the duration of transient Ca^{2+} release events, which in ICC means shorter electrical slow waves due to rapid buffering of released cytosolic Ca^{2+} and repolarization of plasma membrane as Ca^{2+} -activated Anol channels close. Our observations match these predictions, raising extracellular HCO_3^- to 100mM will alkalinize the cytosol on entry through NBCe1, which we found reversibly increased the frequency and shortened the duration of the slow waves. Removing HCO_3^- will acidify the cytosol due to efflux of HCO_3^- through NBCe1, which we found reduced slow wave frequency, slowed the rise time to peak amplitude and increased slow wave duration. These changes in slow wave properties due to modulation of intracellular Ca^{2+} handling are modest compared to the effect of completely blocking intracellular Ca^{2+} release or reuptake but consistent with studies that identified the central role of Ca^{2+} in slow wave generation^{20,23}. It is also probable that altered intracellular pH could modify the activity

of other molecules linked to slow wave generation including the T-type Ca^{2+} channel and the NKCC1 transporter but data are not available on how or whether they are affected. The other notable observation was that increasing and reducing HCO_3^- concentrations resulted in little change to membrane voltage at the peak of the slow wave events, even though it is likely that peak intracellular Ca^{2+} concentrations changed in response to changes in intracellular pH, as it does in other cell types³³. This demonstrates that Ano1 activation, which sets the plateau potential of the slow wave by driving the ICC membrane potential to the zero current potential for small anions, is not significantly affected by intracellular pH. Furthermore, it shows that the reversal potential for Ano1-mediated anion conductances is not modified by replacing Cl^- with HCO_3^- , consistent with the high HCO_3^- permeability of Ano1 channels⁵⁵⁻⁵⁷. Our proposed model for how HCO_3^- transport contributes to the electrical activity in the mouse small intestine is illustrated in the graphical abstract provided with this article (Supplementary Figure 1).

The rapid and profound effects of substituting Na^+ with Li^+ on smooth muscle membrane potential and slow wave activity, while consistent with the inability of NBCe1 to co-transport Li^+ and $\text{HCO}_3^-/\text{CO}_3^{2-}$ ⁴⁸, were considerably greater than the simple effect of removing HCO_3^- . Voltage-gated Na^+ currents, while present in human intestinal ICC, have not been found in rodent smooth muscle cells^{11, 58} and even if they were present, they are freely permeable to Li^+ , so replacement of Na^+ should not impact any contribution of these channels to slow wave generation. However, Li^+ is not carried by either NCX or NKCC1 activity⁴⁸, and both of these transporters play a role in generation of Ca^{2+} transients that underlie pacemaker activity in ICC from both mouse intestine and rabbit urethra^{28, 29, 59}. The absence of a further effect when we removed HCO_3^- from Li^+ containing solutions was consistent with NBCe1 activity being the major contributor to HCO_3^- transport in ICC-MY and overall our results support a role for plasma membrane Na^+ transport in ICC function.

NBCe1 activity appears to contribute most to HCO_3^- transport when the steady state is disrupted, for example after changing extracellular HCO_3^- . This is evident in the significant effect of S-0859 in reducing changes in smooth muscle membrane potential and slow wave amplitude and frequency in response to removing HCO_3^- . S-0859 produced small changes to baseline electrical activity when applied in normal KRB to the tissue for up to 8 minutes, indicating that NBCe1 may be playing a minimal dynamic role in slow wave generation but is more important for homeostatic regulation of intracellular pH and trans-membrane HCO_3^- distribution. S-0859 at 30 μM is selective for NBCe1 over other plasma membrane transport proteins that contribute to regulation of intracellular pH. For example 10–30 μM S-0859 does not significantly affect NHE activity, $\text{HCO}_3^-/\text{Cl}^-$ exchange, carbonic anhydrase activities or $\text{Na}^+/\text{Ca}^{2+}$ exchange in cardiac ventricular myocytes⁴³. S-0859 does partially inhibit the activity of monocarboxylate transporters (Slc16a1, Slc16a3 and Slc16a7) and the neutral $\text{Na}^+ \text{HCO}_3^-$ transporter NBCn1, Slc4a7^{44, 45} at 50 μM but the mRNA transcripts for these molecules are not significantly enriched in pacemaker ICC-MY of mouse small intestine³⁶. Overall, the effects of S-0859 confirm that NBCe1 activity contributes significantly to pacemaker activity of mouse small intestinal ICC although the activity of other selective ion transport mechanisms also play important roles in this process.

This study identifies pacemaker activity as the principal molecular process modified by HCO_3^- transport in ICC, other studies have shown that elevated intracellular pH in ICC increases coupling between ICC through gap junctions^{60, 61}. We did not observe evidence of irregular slow wave activity following removal of HCO_3^- , which would be consistent with disrupted ICC network function as predicted by a decrease in intracellular pH. Slow wave activity prior to application of 100mM HCO_3^- was consistently regular, so there was no possibility to see any evidence of higher ICC coupling in those experiments.

Overall, these studies identify a component of the cellular physiology of ICC that can be investigated in depth thanks to the development of new tools for altering gene expression and following changes in intracellular Ca^{2+} and pH. The unresolved question is whether NBCe1 is setting global intracellular pH levels or if it contributes to transient or local gradients of pH perhaps due to its voltage dependence. NBCe1 is a molecule that is discretely distributed in polarized cells and it is likely that it is restricted to specific microdomains in the plasma membrane of ICC, possibly adjacent to other molecules including NKCC1²⁹ and the T-type Ca^{2+} channel, *Cacna1b*^{21, 22} that contribute to functional pacemaker units in ICC-MY. Loss of function mutations in SLC4A4 have profound effects on human health^{62, 63} and *Slc4a4*-knockout die shortly after birth⁴² due to systemic acidosis. Linkage of mutations in SLC4A4 to gastrointestinal motility disorders have not been reported but may be evident for mutations that affect one or other of the transcript variants generated from the SLC4A4 gene. In conclusion, NBCe1 is a major contributor to HCO_3^- transport in ICC-MY, which is required for normal pacemaker activity in the small intestine of mice, and likely contributes to gastrointestinal motility patterns.

Supplementary Material

Refer to Web version on PubMed Central for supplementary material.

ACKNOWLEDGEMENTS, FUNDING, DISCLOSURES

This work was supported by NIH R01 DK57061 to Dr. Gibbons and Dr. Farrugia, by the Mayo Clinic Center for Cell Signaling in Gastroenterology P30DK084567, and Grant No. 81670492 from the National Natural Science Foundation of China to Dr. Lei Sha. We wish to thank the members of the Enteric Neurosciences Program at Mayo Clinic for their support and feedback on this study. None of the authors have any relevant disclosures to declare in respect of this work.

Data Availability Statement:

Data available on request from the authors.

REFERENCES

1. Szurszewski JH. Electrophysiological basis of gastrointestinal motility. In: Johnson LRCJ, Jackson MJ, Jacobson ED & Walsh JH ed. Physiology of the Gastrointestinal Tract. New York: Raven 1987:383–422.
2. Ward SM, Burns AJ, Torihashi S, Sanders KM. Mutation of the proto-oncogene c-kit blocks development of interstitial cells and electrical rhythmicity in murine intestine. J Physiol1994; 480 (Pt 1): 91–7. [PubMed: 7853230]

3. Huizinga JD, Thuneberg L, Kluppel M, Malysz J, Mikkelsen HB, Bernstein A. W/kit gene required for interstitial cells of Cajal and for intestinal pacemaker activity. *Nature*1995; 373: 347–9. [PubMed: 7530333]
4. Komuro T. Comparative morphology of interstitial cells of Cajal: ultrastructural characterization. *Microsc Res Tech*1999; 47: 267–85. [PubMed: 10602287]
5. Rich A, Leddon SA, Hess SL, Gibbons SJ, Miller S, Xu X, Farrugia G. Kit-like immunoreactivity in the zebrafish gastrointestinal tract reveals putative ICC. *Dev Dyn*2007; 236: 903–11. [PubMed: 17295318]
6. Sha L, Farrugia G, Harmsen WS, Szurszewski JH. Membrane potential gradient is carbon monoxide-dependent in mouse and human small intestine. *Am J Physiol Gastrointest Liver Physiol*2007; 293: G438–45. [PubMed: 17510199]
7. Ward SM, Sanders KM. Interstitial cells of Cajal: primary targets of enteric motor innervation. *Anat Rec*2001; 262: 125–35. [PubMed: 11146435]
8. Ward SM, McLaren GJ, Sanders KM. Interstitial cells of Cajal in the deep muscular plexus mediate enteric motor neurotransmission in the mouse small intestine. *J Physiol*2006; 573: 147–59. [PubMed: 16513671]
9. Gibbons SJ. Not just there to fill space: profound observations on interstitial cells of Cajal in the gastric fundus. *J Physiol*2018; 596: 1535–6. [PubMed: 29508395]
10. Won KJ, Sanders KM, Ward SM. Interstitial cells of Cajal mediate mechanosensitive responses in the stomach. *Proc Natl Acad Sci U S A*2005; 102: 14913–8. [PubMed: 16204383]
11. Strege PR, Ou Y, Sha L, Rich A, Gibbons SJ, Szurszewski JH, Sarr MG, Farrugia G. Sodium current in human intestinal interstitial cells of Cajal. *Am J Physiol Gastrointest Liver Physiol*2003; 285: G1111–21. [PubMed: 12893628]
12. Sato D, Lai ZF, Tokutomi N, Tokutomi Y, Maeda H, Nishikawa S, Nishikawa S, Ogawa M, et al. Impairment of Kit-dependent development of interstitial cells alters contractile responses of murine intestinal tract. *Am J Physiol*1996; 271: G762–71. [PubMed: 8944689]
13. Ordog T, Takayama I, Cheung WK, Ward SM, Sanders KM. Remodeling of networks of interstitial cells of Cajal in a murine model of diabetic gastroparesis. *Diabetes*2000; 49: 1731–9. [PubMed: 11016458]
14. Choi KM, Gibbons SJ, Nguyen TV, Stoltz GJ, Lurken MS, Ordog T, Szurszewski JH, Farrugia G. Heme oxygenase-1 protects interstitial cells of Cajal from oxidative stress and reverses diabetic gastroparesis. *Gastroenterology*2008; 135: 2055–64, 64 e1–2. [PubMed: 18926825]
15. Wedel T, Spiegler J, Soellner S, Roblick UJ, Schiedeck TH, Bruch HP, Krammer HJ. Enteric nerves and interstitial cells of Cajal are altered in patients with slow-transit constipation and megacolon. *Gastroenterology*2002; 123: 1459–67. [PubMed: 12404220]
16. Lyford GL, He CL, Soffer E, Hull TL, Strong SA, Senagore AJ, Burgart LJ, Young-Fadok T, et al. Pan-colonic decrease in interstitial cells of Cajal in patients with slow transit constipation. *Gut*2002; 51: 496–501. [PubMed: 12235070]
17. He CL, Burgart L, Wang L, Pemberton J, Young-Fadok T, Szurszewski J, Farrugia G. Decreased interstitial cell of cajal volume in patients with slow-transit constipation. *Gastroenterology*2000; 118: 14–21. [PubMed: 10611149]
18. Grover M, Farrugia G, Lurken MS, Bernard CE, Fausone-Pellegrini MS, Smyrk TC, Parkman HP, Abell TL, et al. Cellular changes in diabetic and idiopathic gastroparesis. *Gastroenterology*2011; 140: 1575–85 e8. [PubMed: 21300066]
19. O’Grady G, Angeli TR, Du P, Lahr C, Lammers W, Windsor JA, Abell TL, Farrugia G, et al. Abnormal initiation and conduction of slow-wave activity in gastroparesis, defined by high-resolution electrical mapping. *Gastroenterology*2012; 143: 589–98 e3. [PubMed: 22643349]
20. Ward SM, Baker SA, de Faoite A, Sanders KM. Propagation of slow waves requires IP3 receptors and mitochondrial Ca²⁺ uptake in canine colonic muscles. *J Physiol*2003; 549: 207–18. [PubMed: 12665604]
21. Gibbons SJ, Strege PR, Lei S, Roeder JL, Mazzone A, Ou Y, Rich A, Farrugia G. The alpha1H Ca²⁺ channel subunit is expressed in mouse jejunal interstitial cells of Cajal and myocytes. *J Cell Mol Med*2009; 13: 4422–31. [PubMed: 19413888]

22. Zheng H, Park KS, Koh SD, Sanders KM. Expression and function of a T-type Ca²⁺ conductance in interstitial cells of Cajal of the murine small intestine. *Am J Physiol Cell Physiol*2014; 306: C705–13. [PubMed: 24477235]
23. Zheng H, Drumm BT, Earley S, Sung TS, Koh SD, Sanders KM. SOCE mediated by STIM and Orai is essential for pacemaker activity in the interstitial cells of Cajal in the gastrointestinal tract. *Sci Signal*2018; 11.
24. Singh RD, Gibbons SJ, Saravanaperumal SA, Du P, Hennig GW, Eisenman ST, Mazzone A, Hayashi Y, et al. Ano1, a Ca²⁺-activated Cl⁻ channel, coordinates contractility in mouse intestine by Ca²⁺ transient coordination between interstitial cells of Cajal. *J Physiol*2014; 592: 4051–68. [PubMed: 25063822]
25. Malysz J, Gibbons SJ, Saravanaperumal SA, Du P, Eisenman ST, Cao C, Oh U, Saur D, et al. Conditional genetic deletion of Ano1 in interstitial cells of Cajal impairs Ca²⁺ transients and slow waves in adult mouse small intestine. *Am J Physiol Gastrointest Liver Physiol*2017; 312: G228–G45. [PubMed: 27979828]
26. Hwang SJ, Blair PJ, Britton FC, O’Driscoll KE, Hennig G, Bayguinov YR, Rock JR, Harfe BD, et al. Expression of anoctamin 1/TMEM16A by interstitial cells of Cajal is fundamental for slow wave activity in gastrointestinal muscles. *J Physiol*2009; 587: 4887–904. [PubMed: 19687122]
27. Ward SM, Ordog T, Koh SD, Baker SA, Jun JY, Amberg G, Monaghan K, Sanders KM. Pacemaking in interstitial cells of Cajal depends upon calcium handling by endoplasmic reticulum and mitochondria. *J Physiol*2000; 525Pt 2: 355–61. [PubMed: 10835039]
28. Zheng H, Drumm BT, Zhu MH, Xie Y, O’Driscoll KE, Baker SA, Perrino BA, Koh SD, et al. Na⁺/Ca²⁺ exchange and pacemaker activity of interstitial cells of Cajal. *Front Physiol*2020; 11: 230. [PubMed: 32256387]
29. Wouters M, De Laet A, Donck LV, Delpire E, van Bogaert PP, Timmermans JP, de Kerchove d’Exaerde A, Smans K, et al. Subtractive hybridization unravels a role for the ion cotransporter NKCC1 in the murine intestinal pacemaker. *Am J Physiol Gastrointest Liver Physiol*2006; 290: G1219–27. [PubMed: 16123204]
30. Tsukioka M, Iino M, Endo M. pH dependence of inositol 1,4,5-trisphosphate-induced Ca²⁺ release in permeabilized smooth muscle cells of the guinea-pig. *J Physiol*1994; 475: 369–75. [PubMed: 8006822]
31. De Smet P, Parys JB, Vanlingen S, Bultynck G, Callewaert G, Galione A, De Smedt H, Missiaen L. The relative order of IP₃ sensitivity of types 1 and 3 IP₃ receptors is pH dependent. *Pflugers Arch*1999; 438: 154–8. [PubMed: 10370101]
32. Danthuluri NR, Kim D, Brock TA. Intracellular alkalinization leads to Ca²⁺ mobilization from agonist-sensitive pools in bovine aortic endothelial cells. *J Biol Chem*1990; 265: 19071–6. [PubMed: 2172243]
33. Li S, Hao B, Lu Y, Yu P, Lee HC, Yue J. Intracellular alkalinization induces cytosolic Ca²⁺ increases by inhibiting sarco/endoplasmic reticulum Ca²⁺-ATPase (SERCA). *PLoS One*2012; 7: e31905. [PubMed: 22384096]
34. Wienbeck M, Golenhofen K, Lammel E. The effects of CO₂ and pH on the spontaneous activity of the taenia coli of guinea-pig. *Pflügers Archiv*1972; 334: 181–92. [PubMed: 4672129]
35. McSwiney BA, Newton WH. Reaction of smooth muscle to the h-ion concentration. *J Physiol*1927; 63: 51–60. [PubMed: 16993866]
36. Chen H, Ordog T, Chen J, Young DL, Bardsley MR, Redelman D, Ward SM, Sanders KM. Differential gene expression in functional classes of interstitial cells of Cajal in murine small intestine. *Physiol Genomics*2007; 31: 492–509. [PubMed: 17895395]
37. Romero MF, Chen AP, Parker MD, Boron WF. The SLC4 family of bicarbonate (HCO₃⁻) transporters. *Mol Aspects Med*2013; 34: 159–82. [PubMed: 23506864]
38. Rickmann M, Orłowski B, Heupel K, Roussa E. Distinct expression and subcellular localization patterns of Na⁺/HCO₃⁻ cotransporter (SLC 4A4) variants NBCe1-A and NBCe1-B in mouse brain. *Neuroscience*2007; 146: 1220–31. [PubMed: 17433553]
39. Ruffin VA, Salameh AI, Boron WF, Parker MD. Intracellular pH regulation by acid-base transporters in mammalian neurons. *Front Physiol*2014; 5: 43. [PubMed: 24592239]

40. Wang HS, Chen Y, Vairamani K, Shull GE. Critical role of bicarbonate and bicarbonate transporters in cardiac function. *World J Biol Chem*2014; 5: 334–45. [PubMed: 25225601]
41. Kurtz I. NBCe1 as a model carrier for understanding the structure–function properties of Na(+)-coupled SLC4 transporters in health and disease. *Pflugers Arch*2014; 466: 1501–16. [PubMed: 24515290]
42. Gawenis LR, Bradford EM, Prasad V, Lorenz JN, Simpson JE, Clarke LL, Woo AL, Grisham C, et al. Colonic anion secretory defects and metabolic acidosis in mice lacking the NBC1 Na⁺/HCO₃⁻ cotransporter. *J Biol Chem*2007; 282: 9042–52. [PubMed: 17192275]
43. Ch'en FF, Villafuerte FC, Swietach P, Cobden PM, Vaughan-Jones RD. S0859, an N-cyanosulphonamide inhibitor of sodium-bicarbonate cotransport in the heart. *Br J Pharmacol*2008; 153: 972–82. [PubMed: 18204485]
44. Jiang S, Wang X, Wei J, Zhang G, Zhang J, Xie P, Xu L, Wang L, et al. NaHCO₃ Dilates Mouse Afferent Arteriole Via Na(+)/HCO₃(-) Cotransporters NBCs. *Hypertension*2019; 74: 1104–12. [PubMed: 31522618]
45. Heidtmann H, Ruminot I, Becker HM, Deitmer JW. Inhibition of monocarboxylate transporter by N-cyanosulphonamide S0859. *Eur J Pharmacol*2015; 762: 344–9. [PubMed: 26027796]
46. Saravanaperumal SA, Gibbons SJ, Malysz J, Sha L, Linden DR, Szurszewski JH, Farrugia G. Extracellular Cl(-) regulates electrical slow waves and setting of smooth muscle membrane potential by interstitial cells of Cajal in mouse jejunum. *Exp Physiol*2018; 103: 40–57. [PubMed: 28971566]
47. Colmenares Aguilar MG, Mazzone A, Eisenman ST, Strega PR, Bernard CE, Holmes HL, Romero MF, Farrugia G, et al. Expression of the regulated isoform of the electrogenic Na(+)/HCO₃(-) cotransporter, NBCe1, is enriched in pacemaker interstitial cells of Cajal. *Am J Physiol Gastrointest Liver Physiol*2021; 320: G93–G107. [PubMed: 33112159]
48. Sciortino CM, Romero MF. Cation and voltage dependence of rat kidney electrogenic Na(+)-HCO₃(-) cotransporter, rNBC, expressed in oocytes. *Am J Physiol*1999; 277: F611–23. [PubMed: 10516286]
49. Turovsky E, Theparambil SM, Kasymov V, Deitmer JW, Del Arroyo AG, Ackland GL, Corneveaux JJ, Allen AN, et al. Mechanisms of CO₂/H⁺ Sensitivity of Astrocytes. *J Neurosci*2016; 36: 10750–8. [PubMed: 27798130]
50. Colmenares Aguilar MG, Mazzone A, Zhao W, Strega PR, Eisenman ST, Silva JM, Sha L, Shull GE, et al. Immunoreactivity for the Na⁺/HCO₃⁻ cotransporter (NBCe1, Slc4a4) in pacemaker interstitial cells of Cajal is selectively reduced by knocking down Slc4a4 gene expression using an ETV1-cre driver in mouse. *Neurogastroenterol Motil*2019; 31.
51. Wray S. Smooth muscle intracellular pH: measurement, regulation, and function. *Am J Physiol*1988; 254: C213–25. [PubMed: 3279796]
52. Casey JR, Grinstein S, Orlowski J. Sensors and regulators of intracellular pH. *Nat Rev Mol Cell Biol*2010; 11: 50–61. [PubMed: 19997129]
53. Haumann J, Camara AKS, Gadicherla AK, Navarro CD, Boelens AD, Blomeyer CA, Dash RK, Boswell MR, et al. Slow Ca²⁺ Efflux by Ca²⁺/H⁺ Exchange in Cardiac Mitochondria Is Modulated by Ca²⁺ Re-uptake via MCU, Extra-Mitochondrial pH, and H⁺ Pumping by FOF1-ATPase. *Front Physiol*2018; 9: 1914. [PubMed: 30804812]
54. Poburko D, Santo-Domingo J, Demareux N. Dynamic regulation of the mitochondrial proton gradient during cytosolic calcium elevations. *J Biol Chem*2011; 286: 11672–84. [PubMed: 21224385]
55. Jung J, Nam JH, Park HW, Oh U, Yoon JH, Lee MG. Dynamic modulation of ANO1/TMEM16A HCO₃(-) permeability by Ca²⁺/calmodulin. *Proc Natl Acad Sci U S A*2013; 110: 360–5. [PubMed: 23248295]
56. Yang YD, Cho H, Koo JY, Tak MH, Cho Y, Shim WS, Park SP, Lee J, et al. TMEM16A confers receptor-activated calcium-dependent chloride conductance. *Nature*2008; 455: 1210–5. [PubMed: 18724360]
57. Qu Z, Hartzell HC. Anion permeation in Ca²⁺-activated Cl(-) channels. *J Gen Physiol*2000; 116: 825–44. [PubMed: 11099350]

58. Strege PR, Mazzone A, Kraichely RE, Sha L, Holm AN, Ou Y, Lim I, Gibbons SJ, et al. Species dependent expression of intestinal smooth muscle mechanosensitive sodium channels. *Neurogastroenterol Motil* 2007; 19: 135–43. [PubMed: 17244168]
59. Bradley E, Hollywood MA, Johnston L, Large RJ, Matsuda T, Baba A, McHale NG, Thornbury KD, et al. Contribution of reverse Na⁺-Ca²⁺ exchange to spontaneous activity in interstitial cells of Cajal in the rabbit urethra. *J Physiol* 2006; 574: 651–61. [PubMed: 16728449]
60. Belzer V, Kobil T, Rich A, Hanani M. Intercellular coupling among interstitial cells of Cajal in the guinea pig small intestine. *Cell Tissue Res* 2002; 307: 15–21. [PubMed: 11810310]
61. Kobil T, Szurszewski JH, Farrugia G, Hanani M. Coupling and innervation patterns of interstitial cells of Cajal in the deep muscular plexus of the guinea-pig. *Neurogastroenterol Motil* 2003; 15: 635–41. [PubMed: 14651599]
62. Horita S, Yamada H, Inatomi J, Moriyama N, Sekine T, Igarashi T, Endo Y, Dasouki M, et al. Functional analysis of NBC1 mutants associated with proximal renal tubular acidosis and ocular abnormalities. *J Am Soc Nephrol* 2005; 16: 2270–8. [PubMed: 15930088]
63. Igarashi T, Inatomi J, Sekine T, Cha SH, Kanai Y, Kunimi M, Tsukamoto K, Satoh H, et al. Mutations in SLC4A4 cause permanent isolated proximal renal tubular acidosis with ocular abnormalities. *Nat Genet* 1999; 23: 264–6. [PubMed: 10545938]

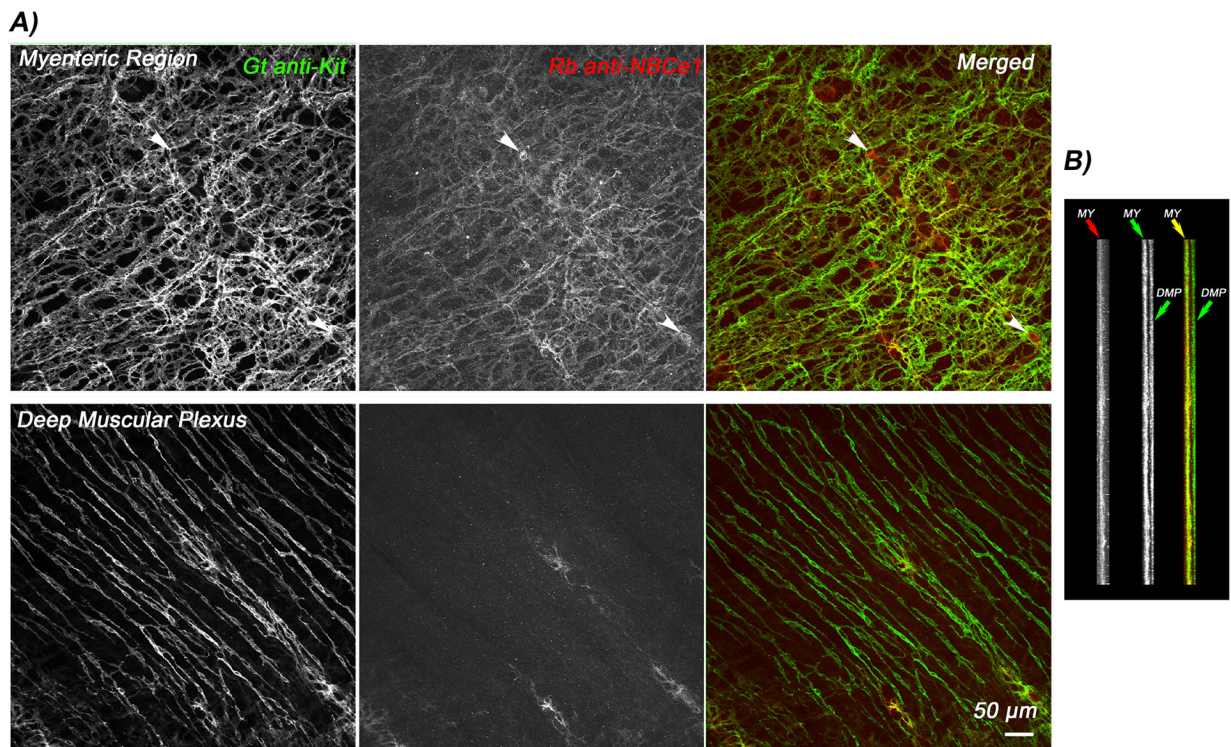


Figure 1. NBCe1-immunoreactivity (NBCe1-IR) in myenteric interstitial cells of Cajal (ICC-MY) of the mouse small intestine.

Flattened projection images generated from a stack of confocal images through the full thickness of the small intestinal muscularis propria shown en face from the myenteric region and deep muscular plexus (A). ICC-MY are doubly labelled for KIT and NBCe1 (upper panels) whereas ICC-DMP are NBCe1-negative (lower panels). A small number of myenteric neurons, indicated by white arrowheads are NBCe1-positive but Kit-negative. Panel B) shows the confocal stack in cross section showing that Kit and NBCe1 only co-localizes in the myenteric region. Images are representative of observations from independent experiments on tissues from N=3 mice.

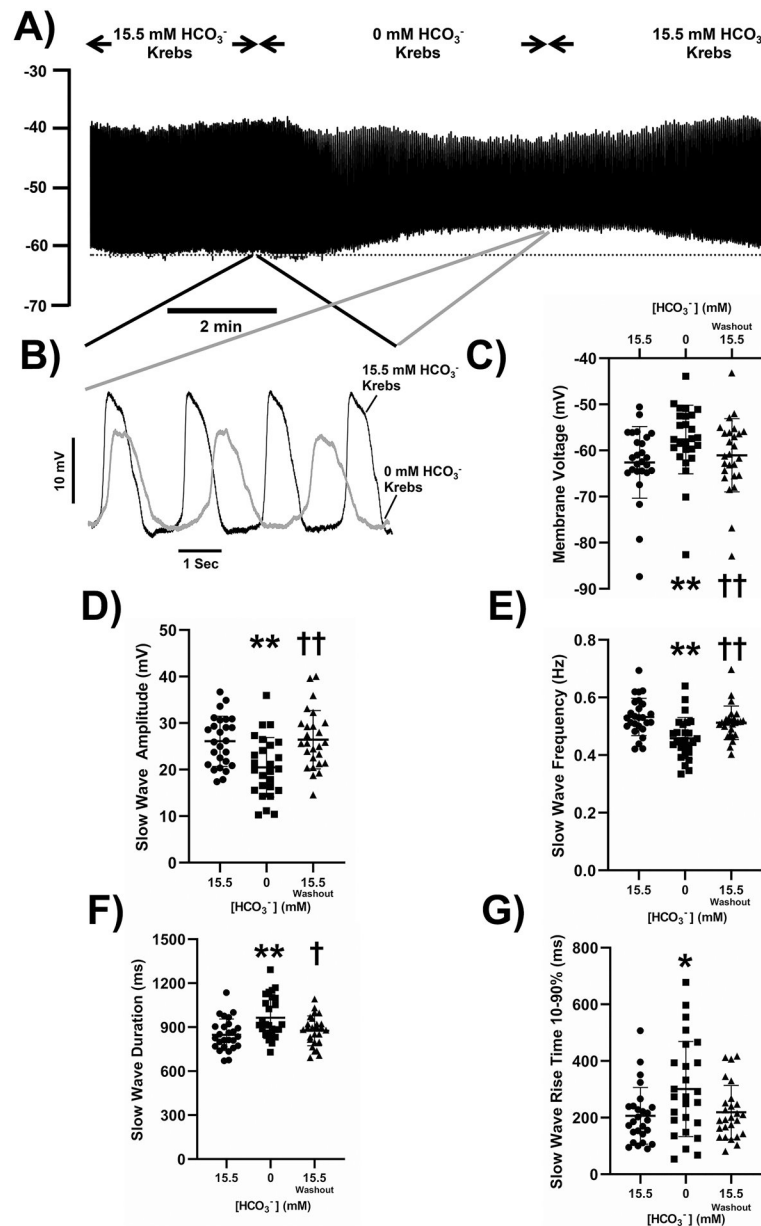


Figure 2: The effect of removing HCO_3^- from the extracellular recording solution on electrical slow wave activity in the mouse small intestine.

Removal of HCO_3^- reversibly caused membrane potential depolarization (A) and smaller, lower frequency slow waves (B). Pooled analysis showing reproducible and statistically significant effects on membrane potential (C), slow wave amplitude (D), slow wave frequency (E), slow wave duration (width at half peak amplitude, F) and slow wave rise time from 10–90% of peak amplitude (G). The dotted line in panel A indicates the baseline membrane voltage to which the traces in panel B are aligned and the regions of the traces shown in panel B are linked by lines to the corresponding regions in panel A. Points represent data from individual mice calculated as means of recordings from each tissue. Whiskers are means \pm STDEV. ** - $P < 0.001$ vs 15.5 mM HCO_3^- , * - $P < 0.05$ vs 15.5 mM

HCO_3^- , $\dagger\dagger$ - $P < 0.001$ vs 0 mM HCO_3^- , \dagger - $P < 0.05$ vs 0 mM HCO_3^- . Repeated measures one-way ANOVA with Tukey's post test. $N = 26$ mice.

Author Manuscript

Author Manuscript

Author Manuscript

Author Manuscript

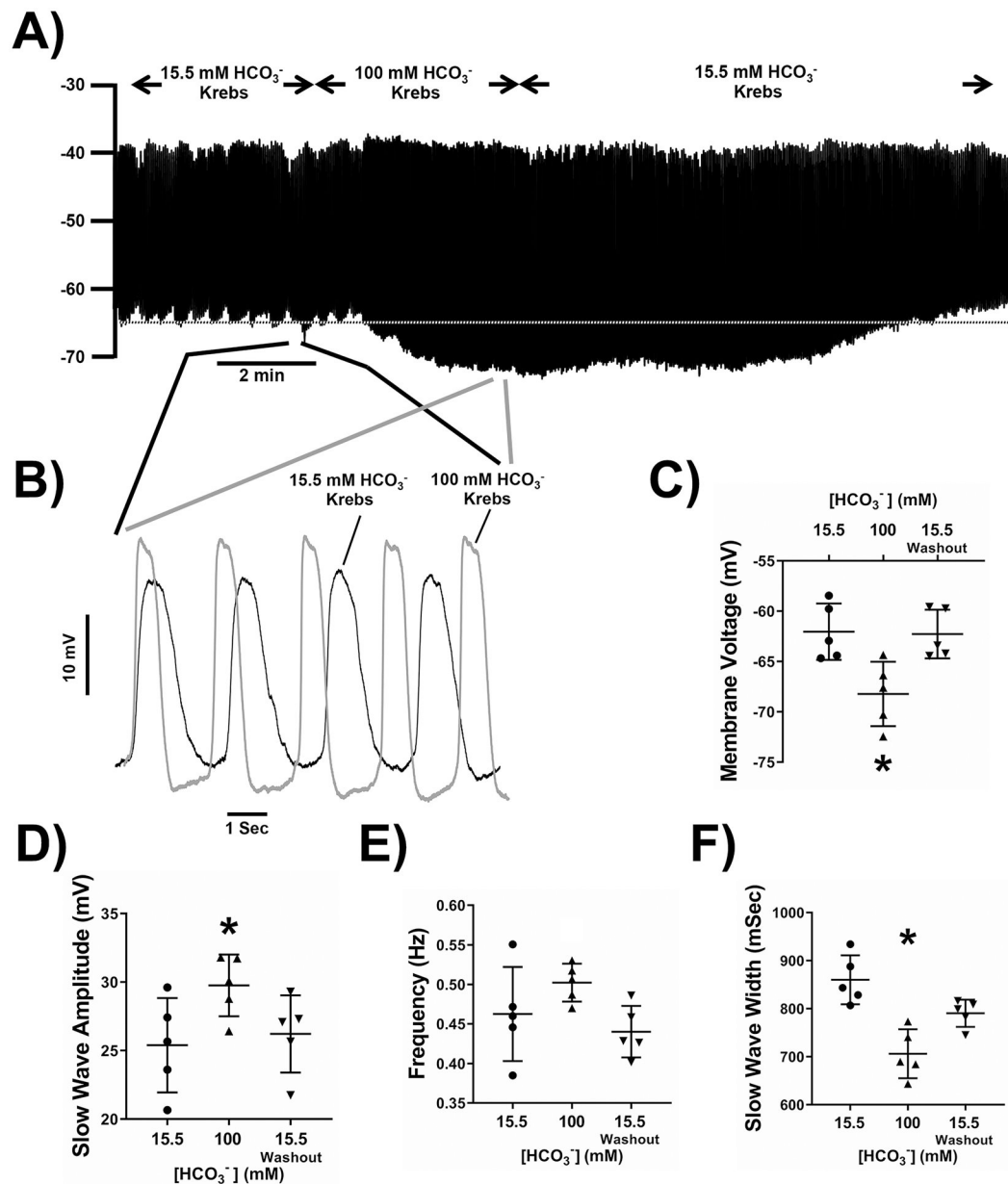


Figure 3: The effect of 100 mM HCO₃⁻ concentration in the extracellular recording solution on electrical slow wave activity in the mouse small intestine.

100 mM HCO₃⁻ reversibly caused membrane potential hyperpolarization (A) and larger, faster frequency slow waves (B). Pooled analysis showing reproducible and statistically significant effects on membrane potential (C), slow wave amplitude (D), slow wave frequency (E), slow wave duration (width at half peak amplitude, F) and slow wave rise time from 10–90% of peak amplitude (G). The dotted line in panel A indicates the baseline membrane voltage to which the traces in panel B are aligned and the regions of the traces shown in panel B are linked by lines to the corresponding regions in panel A. Points represent data from individual mice calculated as means of recordings from each tissue. Whiskers are means ± STDEV. * - P < 0.05 vs 15.5 mM HCO₃⁻, † - P < 0.05 vs 100 mM

HCO₃⁻. Repeated measures one-way ANOVA with Tukey's post test. n = 17 cells from N = 5 mice.

Author Manuscript

Author Manuscript

Author Manuscript

Author Manuscript

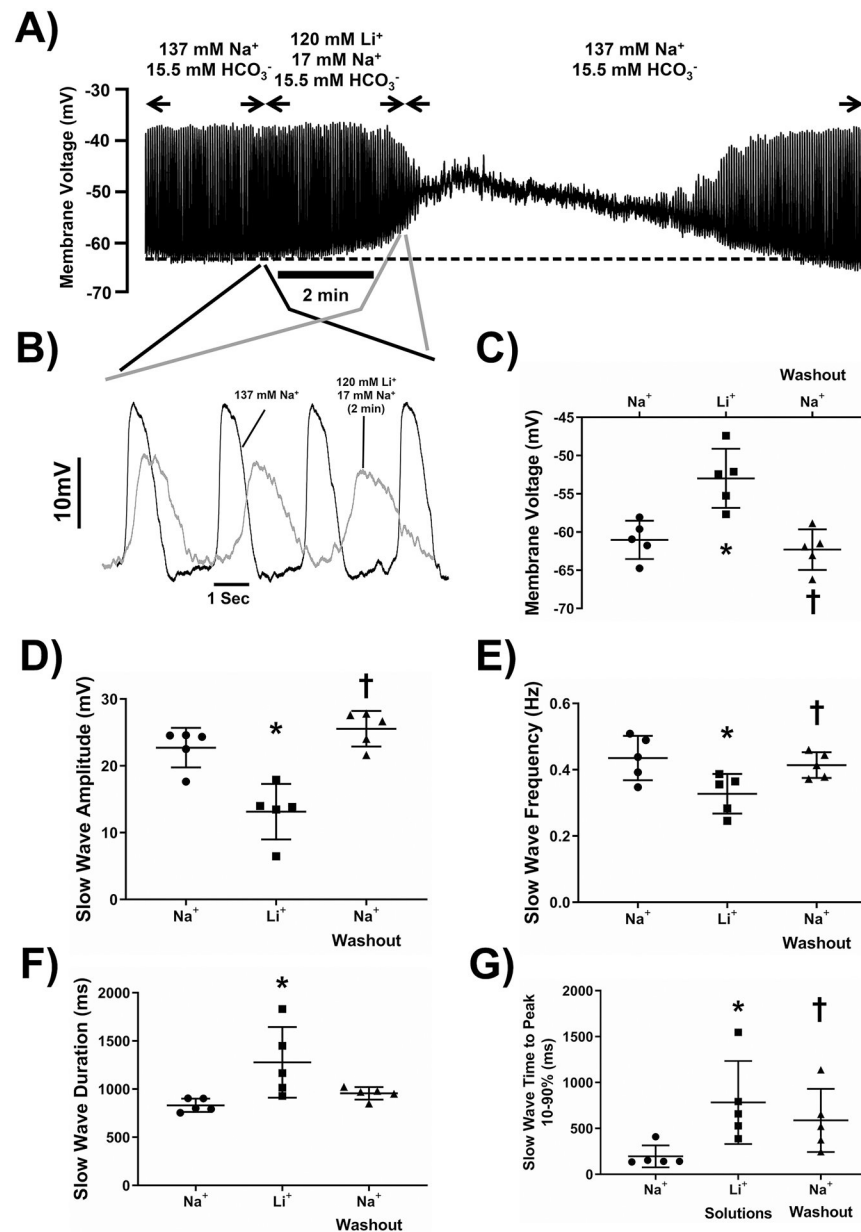


Figure 4: The effect of replacing 120 mM NaCl with LiCl in the extracellular recording solution on electrical slow wave activity in the mouse small intestine.

Replacement of 120 mM of NaCl with equimolar LiCl in the extracellular solution reversibly caused membrane potential depolarization (A) and lower amplitude, longer duration, slower frequency slow waves (B). Pooled analysis showing reproducible and statistically significant effects on membrane potential (C), slow wave amplitude (D), slow wave frequency (E), slow wave duration (width at half peak amplitude, F) and slow wave rise time from 10–90% of peak amplitude (G). Points represent data from individual mice calculated as means of recordings from each tissue. The dotted line in panel A indicates the baseline membrane voltage to which the traces in panel B are aligned and the regions of the traces shown in panel B are linked by lines to the corresponding regions in panel A. Whiskers are means ± STDEV. * - P < 0.05 vs Na⁺-containing Krebs Ringer solution, † -

$P < 0.05$ Washout vs Li^+ -containing solutions. Repeated measures one-way ANOVA with Tukey's post test. $n = 19$ cells from $N = 5$ mice.

Author Manuscript

Author Manuscript

Author Manuscript

Author Manuscript

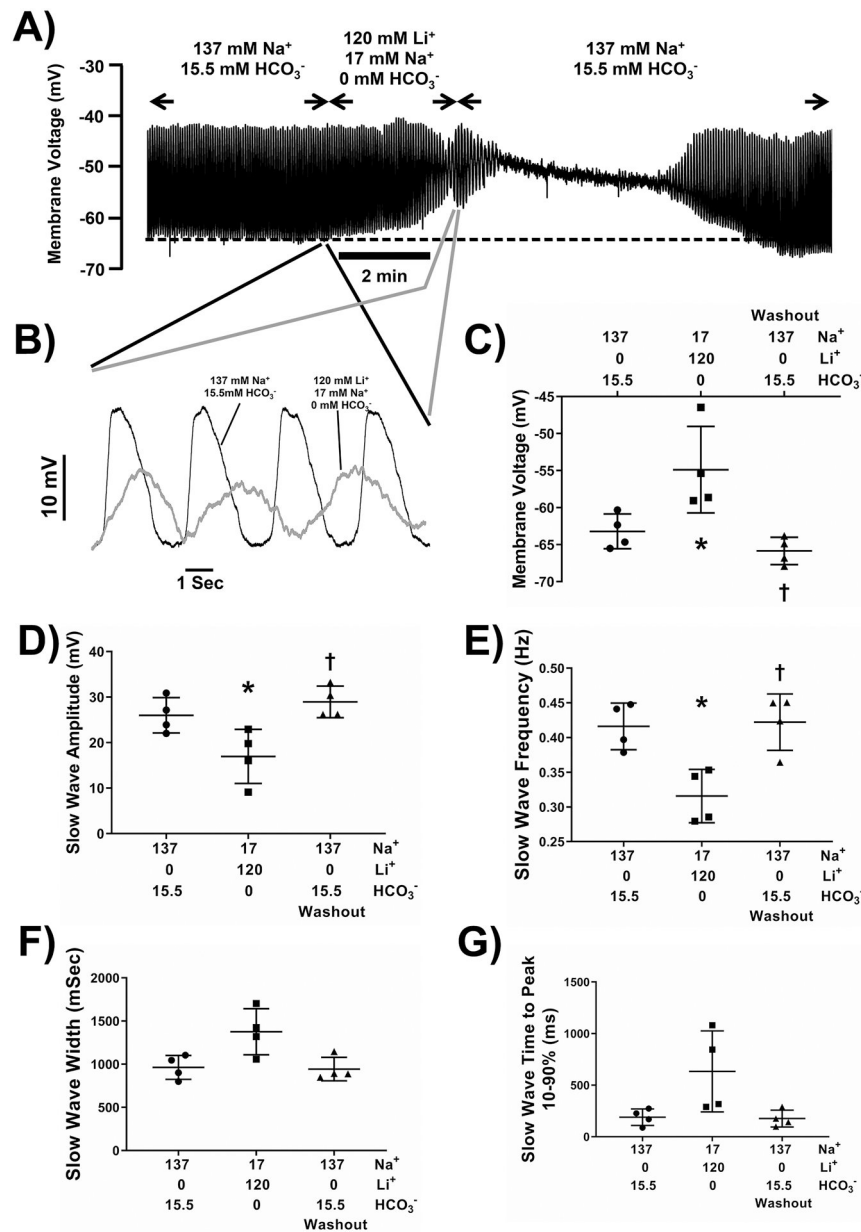


Figure 5: The effect of replacing 120 mM NaCl with LiCl and removing HCO₃⁻ from the extracellular recording solution on electrical slow wave activity in the mouse small intestine. Replacement of 120 mM of NaCl with equimolar LiCl in 0 HCO₃⁻ extracellular solution reversibly caused membrane potential depolarization (A) and lower amplitude, slower frequency slow waves (B). Pooled analysis showing reproducible and statistically significant effects on membrane potential (C), slow wave amplitude and (D), slow wave frequency (E). Slow wave duration (width at half peak amplitude (F), and slow wave rise time from 10–90% of peak amplitude (G) were slightly longer. The dotted line in panel A indicates the baseline membrane voltage to which the traces in panel B are aligned and the regions of the traces shown in panel B are linked by lines to the corresponding regions in panel A. Points represent data from individual mice calculated as means of recordings from each tissue. Whiskers are means ± STDEV. * - P < 0.05 vs Na⁺-containing Krebs Ringer solution,

† - $P < 0.05$ Washout vs Li^+ -containing solutions. Repeated measures one-way ANOVA with Tukey's post test. $n = 14$ cells from $N = 4$ mice.

Author Manuscript

Author Manuscript

Author Manuscript

Author Manuscript

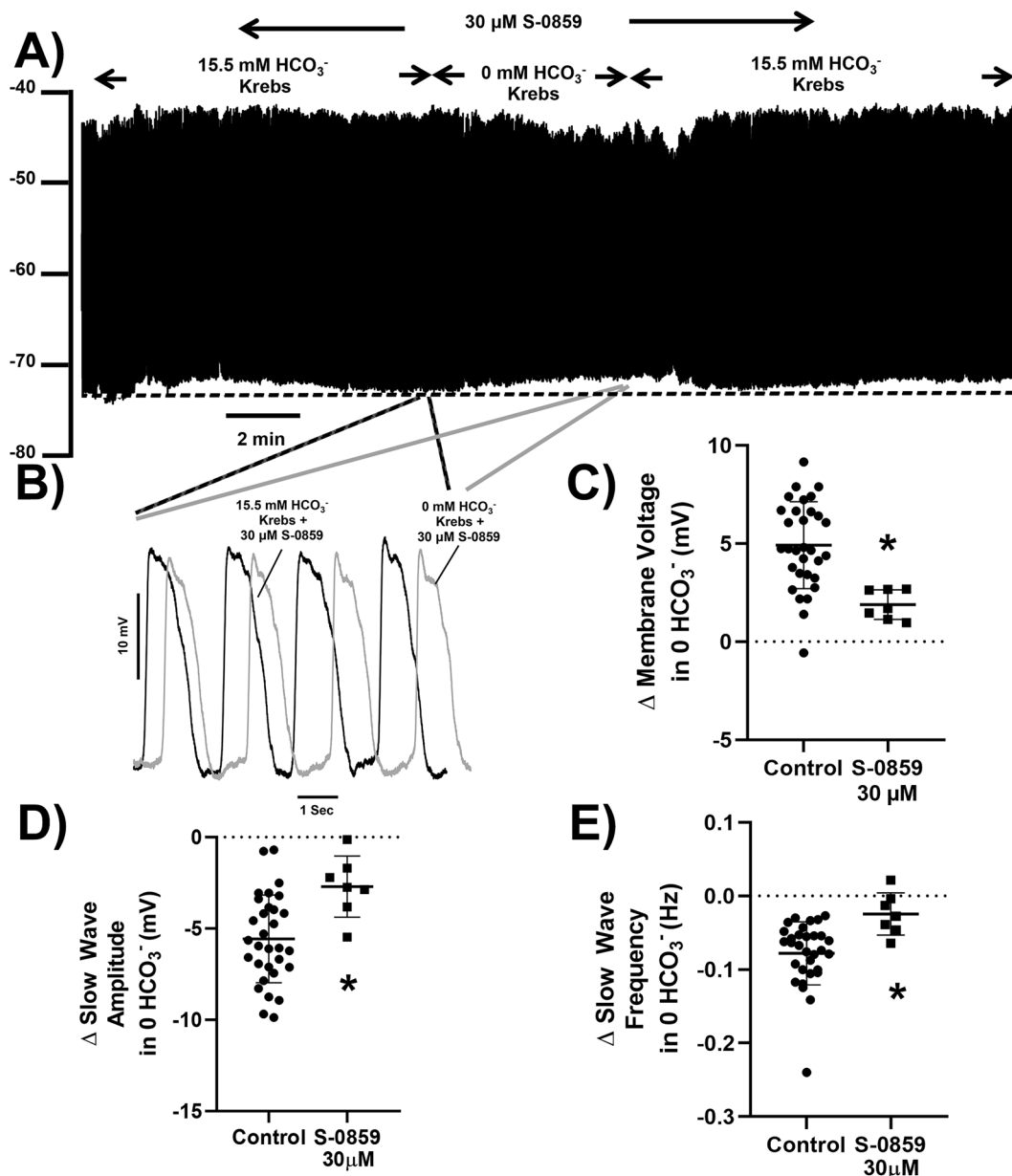


Figure 6: The effect of removing HCO₃⁻ from the extracellular recording solution in the presence of the NBCe1 inhibitor S-0859 on electrical slow wave activity in the mouse small intestine.

Incubation of tissue with 30 μM of the NBCe1 inhibitor, S-0859, caused a small membrane potential hyperpolarization alone and reduced the effect of removing HCO₃⁻ on membrane potential depolarization (A) and electrical slow wave activity (B). Pooled analysis showing reproducible and statistically smaller effects on membrane potential (C), slow wave amplitude (D), and slow wave frequency (E) of switching from 15.5 mM to 0 mM HCO₃⁻. The dotted line in panel A indicates the baseline membrane voltage to which the traces in panel B are aligned and the regions of the traces shown in panel B are linked by lines to the corresponding regions in panel A. Points represent data from individual mice calculated as means of recordings from each tissue, n = 31 cells from N = 26 mice for control and n = 24

cells from N = 7 mice in presence of S-0859. Whiskers are means \pm STDEV. * P < 0.05 vs effect in absence of S-0859 (Control), unpaired Student's t test.

Author Manuscript

Author Manuscript

Author Manuscript

Author Manuscript

Table 1:
Constituents of extracellular solutions used for electrical recordings.

Solutions ② - ⑥ were adjusted pH to 7.4 at 37°C with 1M NaOH. Solution ① reached equilibrium at pH 7.35–7.45 when gassed for 1 hour at 37°C with 97% O₂: 3%CO₂ and was not adjusted further. The osmolarity of the solutions was confirmed to be 310 ± 5 mOsm L⁻¹ at equilibrium.

	① 15.5mM HCO ₃ ⁻	② 15.5mM HCO ₃ ⁻ w HEPES	③ HCO ₃ ⁻ -free	④ 100mM HCO ₃ ⁻	⑤ Low Na ⁺ w. Li ⁺	⑥ Low Na ⁺ w. Li ⁺ HCO ₃ ⁻ -free
NaCl (mM)	120	120	120	35.5	-	-
LiCl	-	-			120	120
KCl (mM)	5.9	5.9	5.9	5.9	5.9	5.9
NaHCO ₃ (mM)	15.5	15.5	-	100	15.5	-
NaH ₂ PO ₄ (mM)	1.2	1.2	1.2	1.2	1.2	1.2
Glucose (mM)	11.5	11.5	11.5	11.5	11.5	11.5
CaCl ₂ (mM)	2.5	2.5	2.5	2.5	2.5	2.5
MgCl ₂ (mM)	2.56	2.56	2.56	2.56	2.56	2.56
HEPES (mM)	-	15.5	15.5	15.5	15.5	15.5
Gas (O ₂ :CO ₂)	97:3	97:3	100:0	80:20	97:3	100:0